ACS Catalysis

Research Article

pubs.acs.org/acscatalysis

Transformation of Isobutyl Alcohol to Aromatics over Zeolite-Based Catalysts

Lili Yu,[†,‡] Shengjun Huang,*[,†] Shuang Zhang,[†] Zhenni Liu,[†] Wenjie Xin,[†] Sujuan Xie,[†] and Longya Xu*[,†]

[†]State Key Laboratory of Catalysis, Dalian Institute of Chemical Physics, Chinese Academy of Sciences, Dalian 116023, China

[‡]Graduate University of Chinese Academy of Sciences, Beijing 100049, China

Supporting Information

ABSTRACT: One-step transformation of isobutyl alcohol to aromatics (benzene, toluene, and xylene) has been studied in a gas phase, fixed-bed reactor system over several purely acidic zeolites and zeolite-supported metal catalysts. ZSM-5 zeolites give higher aromatics yields (~42 wt %) among the evaluated zeolites, and the Si/Al ratios (Si/Al = 13−43) of ZSM-5 slightly influence their catalytic performances. During the transformation of isobutyl alcohol, large amounts of short alkanes (mainly propane and butane isomers) are also generated on the acidic ZSM-5. To improve the conversion to aromatics, several metal species (Zn, Ga, Mo, La, Ni, Ag, and Pt) are supported on the ZSM-5. The enhancements in aromatics yields (~60 wt %) are observed only on the Zn/ZSM-5 catalysts. The incorporation of Zn species preferentially decreases the strong-strength Brønsted acidity and, thus, suppresses the cracking to C_3 fragments. Moreover, mainly the Zn species at the exchange sites facilitate the recombinative desorption of H_2 and, hence, enhance the reactions toward aromatics. Through these effects, Zn/ZSM-5 catalysts exhibit the remarkably promoted formation of toluene and xylene and inhibit the generation of undesired alkanes products.

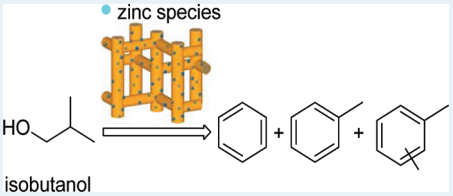

KEYWORDS: *isobutyl alcohol, zeolites, aromatization, zinc species*

1. INTRODUCTION

Aromatics, including benzene, toluene, and xylene (BTX), are large-scale starting feedstocks for numerous chemical industrial processes. Classically, catalytic reforming of naphtha and hydrocarbon pyrolysis are the main routes for the production of these basic aromatics, both of which have been well developed in the petrochemical industry.[1] To match the steadily growing market demand, other processes, such as aromatization of light paraffins, have also been industrialized since the 1990s.[2−5] All of these mature processes are based on the nonrenewable resources of petroleum, coal, and natural gas. However, concerns about the depletion of fossil reserves have stimulated the investigation of sustainable processes for the production of BTX.

Production of aromatics from renewable biomass resources could provide sustainable alternatives to fossil-based processes. Within this trend, the search for suitable biomass resources is primarily crucial for the achievement of a promising process.[6] So far, biomass-derived ethanol, glycerol, *n*-butyl alcohol/acetone and a mixture of C_2−C_5 alcohol have been reported as feedstocks in the production of aromatics.[7−10] From a structure−reactivity viewpoint, ethanol is more suitable for the alcohol-to-olefins process, whereas transformation of glycerol results in a complex product spectrum.[7] The mixture of C_2−C_5 alcohol or *n*-butyl alcohol/acetone suffers from quick deactivation within several hours over the ZSM-5 zeolite.[9,10]

Recently, commercially available biobutanol isomers, obtained from fermentable biomass-derived sugars, have been emerging as a renewable source for fuel.[11,12] Several enterprises have disclosed or announced their commercial processes for the production of biobutanols. Especially, the number of bioisobutyl alcohol producers continues to grow, which ensures availability on a large scale. In addition to its usage in fuel industry, isobutyl alcohol is expected to be a renewable feedstock in the chemical industry. Conceptually, isobutyl alcohol can be regarded as "isobutene hydrate". The dehydrated product of isobutene (or a mixture of butene isomers) can act as platform compounds for the synthesis of various chemicals.[11,12] Among the proposed transformation roadmaps,[11] the dehydration−aromatization of isobutyl alcohol is attractive and integratable with present aromatization process.

Herein, we report the one-step transformation of isobutyl alcohol to aromatics over zeolite-based catalysts. Among the evaluated acidic zeolites, ZSM-5 shows superior catalytic performance for the formation of aromatics due to its shape-selective effect. A large amount of short alkanes (mainly propane and butane isomers) are also generated during the transformation of isobutyl alcohol. To enhance the formation of target BTX aromatics, several dehydrogenation or aromatization-functional promoters (Mo,[13] La,[14] Ga,[15] Zn,[16] Ni,[17] Pt,[18] and Ag[19]) are incorporated to the ZSM-5 zeolite. The enhanced formation of aromatics is observed only on the Zn/ZSM-5 catalysts, which is also accompanied by the suppressed generation of undesired alkanes. The reaction schemes over the ZSM-5 and Zn/ZSM-5 catalysts have been proposed for the transformation of isobutyl alcohol.

Received: January 22, 2012
Revised: May 1, 2012
Published: May 3, 2012

   dx.doi.org/10.1021/cs300048u | ACS Catal. 2012, 2, 1203−1210

2. EXPERIMENTAL SECTION

2.1. Catalysts Preparation. *Acidic Zeolites.* The protonic-form zeolites are commercially available, and their texture parameters are listed in Supporting Information Table S1. The sample is named according to the topology and nominal Si/Al ratio. For example, ZSM-5$^{13.3}$ represents ZSM-5 zeolite with Si/Al ratio of 13.3.

ZSM-5-Supported Metal Catalysts. The supported metal catalysts were prepared by the incipient wetness impregnation method using ZSM-5$^{34.3}$ as support and $Zn(NO_3)_2{\cdot}6H_2O$ (Tianjin Kermel Chemical Reagent Co., Ltd.), $Ga(NO_3)_3{\cdot}H_2O$ (Sterm Chemicals Inc.), $La(NO_3)_3{\cdot}nH_2O$ (n = 2−3) (Shanghai Yuelong Co., Ltd.), $(NH_4)_6Mo_7O_{24}{\cdot}4H_2O$ (Sinopharm Chemical Reagent Co., Ltd.), $AgNO_3$ (Sinopharm Chemical Reagent Co., Ltd.), $Ni(NO_3)_2$ (Tianjin Kermel Chemical Reagent Co., Ltd.), and $H_2PtCl_6{\cdot}6H_2O$ (Shanghai Jiuling Chemical Co., Ltd.) as precursors, respectively. According to the calcination and sequential calcination−reduction procedures, the resulting catalysts are denoted in the following manner: xM/ZSM-5 and xM/ZSM-5-R, where x represents the metal loading in weight percent and R stands for the reduction step, respectively.

xM/ZSM-5: Typically, ZSM-5$^{34.3}$ (4 g) was impregnated with the solution of the precursor (desirable amount of precursor in 10 mL deionized water). The mixture was stirred at room temperature for 8 h and dried in an oven at 60 °C overnight. The dried powder was calcined in flowing air at specific temperatures (500 °C for $Zn(NO_3)_2$/ZSM-5, $Ga(NO_3)_3$/ZSM-5, $La(NO_3)_3$/ZSM-5, and $(NH_4)_6Mo_7O_{24}$/ZSM-5 and 460 °C for $AgNO_3$/ZSM-5) for 4 h.

xM/ZSM-5-R: Typically, ZSM-5$^{34.3}$ (4 g) was impregnated with the solution of the precursor (the desirable amount of precursor in 10 mL deionized water). The mixture was stirred at room temperature for 8 h and dried in an oven at 100 °C overnight. The dried powder was calcined in flowing air at specific temperatures (550 °C for $(NH_4)_6Mo_7O_{24}$/ZSM-5, $Ga(NO_3)_3$/ZSM-5, and $Ni(NO_3)_2$/ZSM-5 and 450 °C for H_2PtCl_6/ZSM-5) and then reduced in H_2 at the same temperatures for 1 h.

2.2. Characterization. X-ray diffraction (XRD) measurements were performed on an X'pert Pro/PANalytical Diffractometer (Cu Kα radiation, 40 kv, 40 mA). The nominal Si/Al ratio was analyzed on a Philips Magix 601X X-ray fluorescence (XRF) spectrometer. Nitrogen adsorption measurements were carried out at −196 °C on a Micromeritics ASAP-2020 analyzer. Prior to analysis, each sample was evacuated at 350 °C for 10 h. The specific surface area was determined by the Brunauer−Emmet−Teller method. Ammonia temperature-programmed desorption (NH_3-TPD) measurements were performed in a homemade flow apparatus using a U-shaped quartz microreactor (4 mm internal diameter). The NH_3-TPD experiment was carried out in the range of 150−600 °C at a ramp rate of 20 °C min^{-1}, and the desorbed ammonia was monitored by a gas chromatograph with a TCD detector.

Pyridine adsorption measurements (Py-IR) were performed on a Thermo Nicolet Nexos 470 instrument. Prior to measurement, a sample (11 mg) was pressed into a self-supported wafer (1.0 MPa, 30 s) and evacuated in an IR cell (attached to a vacuum line) at 450 °C for 1.5 h up to 10^{-2} Pa. After the sample was cooled to room temperature, a spectrum was recorded as background. Subsequently, the wafer was exposed to pyridine vapor (equilibrium vapor at 0 °C) for 20 min, followed by outgassing at 150 °C for 30 min. The IR spectrum was collected after cooling to room temperature.

Diffuse reflectance infrared Fourier transform (DRIFT) spectra were measured with a Thermo Nicolet Nexos 470 instrument (resolution 4 cm^{-1}, integration 20 times) equipped with a Harrick diffuse reflectance attachment. Sample powder (50 mg) was charged in a DRIFT cell with a KBr window and pretreated in flowing dry N_2 flow (>99.99%, 20 mL min^{-1}) at 300 °C for 1 h. After the pretreatment, the sample was cooled, and IR spectra were acquired at 30 °C.

UV−vis spectra were recorded with a JASCO 500 spectrophotometer equipped with a diffuse reflectance attachment. The spectra were recorded under air-exposed conditions in the range of 200−600 nm, and the scan speed was 100 nm min^{-1}. The contribution from the ZSM-5 support has been subtracted from the signal.

2.3. Catalysts Evaluation. The catalytic reaction was carried out in a gas phase, fixed-bed reactor system (stainless steel, 6 mm i.d. and 20 cm in length) at atmospheric pressure. The reaction system includes an HPLC pump, a mass flow controller, an electrically heated preheater section before the entrance to reactor, and an ice bath after the reactor (Supporting Information Figure S1). The catalyst (1.0 g, 20−40 mesh) was packed in the middle zone between two layers of quartz wool, and the thermocouple was fixed to the middle of the external wall of the reactor. The zeolite and xM/ZSM-5 catalysts were pretreated at 480 °C for 1 h in high-purity nitrogen flow (30 mL min^{-1}) before reaction. The xM/ZSM-5-R catalysts were initially pretreated in high-purity hydrogen flow (30 mL min^{-1}) for 1 h, and then switched to high-purity nitrogen flow (30 mL min^{-1}) for 0.5 h. Once the reactor was cooled to 450 °C, liquid isobutyl alcohol was fed using an HPLC pump at a rate of 0.08 mL min^{-1}. The liquid was completely vaporized in the preheated lines (130 °C) before entering the reactor. Effluent was quenched and separated in an ice bath, and gas phase products of C_1−C_5 alkanes and alkenes were analyzed on an online Varian CP-3800 GC equipped with an FID detector and an HP-alumina (PLOT) column (50 m × 0.32 mm). The concentration of H_2 was analyzed by a Shimadzu GC-8A equipped with a TCD detector and a TDX01 molecular sieve column. The collected aqueous and organic phase products were separated by storage in a refrigerator (0 °C) for 10 min. The organic phase products were analyzed by a Varian CP-3800 equipped with an FID detector and a PONA column (30 m × 0.32 mm). The aqueous phase was diluted with ethanol as an internal standard and also analyzed on the above Varian CP-3800 GC.

The overall transformation of isobutyl alcohol comprises complex reaction networks (dehydration, isomerization, oligomerization, cracking, aromatization, etc.). The isobutyl alcohol conversion ($X_{\text{isobutyl alcohol}}$), isobutene conversion ($X_{\text{isobutene}}$), products selectivity (Sel_i), and yield (Y_i) were calculated as following:

$$X_{\text{isobutyl alcohol}} = \frac{m_{\text{inj isobutyl alcohol}} - m_{\text{isobutyl alcohol, aq}} - m_{\text{isobutyl alcohol, org}}}{m_{\text{inj isobutyl alcohol}}} \times 100\% \quad (1)$$

dx.doi.org/10.1021/cs300048u | ACS Catal. 2012, 2, 1203−1210

Table 1. Product Distributions of Isobutyl Alcohol Transformation over Several Zeolites[a]

	product distribution (wt %)																	
catalyst	CH_4	C_2	C_2^{2-}	C_3^0	C_3^{2-}	C_4^0	C_4^{2-}	C_5	C_{6-9}[b]	B[c]	T[d]	EB[e]	*p*-X[f]	*m*-X[g]	*o*-X[h]	C_9^{+}[i]	H_2	ΣA[j]
USY[4.3]	0.1	0	0	0	3.5	1.0	80.1	7.0	5.6	0	0.2	0	0.3	0.2	0.2	1.6	0.1	2.5
ß[31.6]	0.2	0.2	3.7	3.6	19.4	11.4	18.1	16.3	12.0	0.6	2.4	0.5	2.3	1.5	0.6	7.0	0.1	15.0
ZSM-11[26.6]	0.6	0.9	1.8	20.7	2.2	21.4	1.4	6.8	2.0	3.9	14.3	1.0	3.0	7.0	3.1	9.6	0.2	41.9
ZSM-5[13.3]	0.6	0.9	1.6	22.1	1.9	21.3	1.2	7.0	1.7	4.2	15.2	1.0	3.0	7.3	3.2	7.7	0.2	41.6
ZSM-5[34.3]	0.8	1.1	1.0	24.2	2.1	19.3	1.2	6.4	1.4	4.3	15.7	1.0	3.3	7.6	3.4	7.0	0.3	42.3
ZSM-5[42.7]	0.8	1.2	1.6	25.3	1.9	19.0	1.2	5.2	1.2	4.3	15.5	1.0	2.9	7.7	3.3	7.6	0.3	42.3

[a]Reaction conditions: 0.1 MPa, 450 °C, WHSV 3.88 h^{-1}, time-on-stream = 3 h. [b]C_{6-9} alkenes. [c]Benzene. [d]Toluene. [e]Ethylbenzene. [f]*para*-Xylene. [g]*meta*-Xylene. [h]*ortho*-Xylene. [i]C_9 and C_9^+ aromatics. [j]Total yield of aromatics.

Table 2. Product Distributions of Isobutyl Alcohol Transformation over Metal/ZSM-5 Catalysts[a]

	product distribution (wt%)																	
catalyst	CH_4	C_2	C_2^{2-}	C_3	C_3^{2-}	C_4^0	C_4^{2-}	C_5	C_{6-9}[b]	B[c]	T[d]	EB[e]	*p*-X[f]	*m*-X[g]	*o*-X[h]	C_9^{+}[i]	H_2	ΣA[j]
(a)																		
2.3% Zn/ZSM-5	1.2	0.3	2.4	5.5	3.3	12.0	2.4	7.6	2.8	3.8	24.3	2.3	4.6	11.8	4.8	7.8	3.0	59.3
2.1% Ga/ZSM-5	0.9	1.2	1.5	25.2	1.7	18.8	1.1	5.1	1.1	4.6	16.6	1.0	3.3	7.7	3.4	6.3	0.4	42.9
2.4% La/ZSM-5	0.6	0.9	1.9	21.5	2.3	19.0	1.6	6.4	1.9	4.2	16.2	1.2	3.3	8.3	3.6	6.8	0.2	43.6
2.1% Mo/ZSM-5	0.8	1.2	1.4	25.5	1.7	19.2	1.1	5.6	1.1	4.5	15.8	1.0	2.9	7.6	3.2	7.0	0.3	42.0
2.3% Ag/ZSM-5	0.7	1.1	1.2	25.4	1.5	18.8	1.0	5.6	1.2	4.5	16.1	1.1	3.0	8.0	3.4	7.1	0.3	43.2
0.4% Pt/ZSM-5-R	0.7	1.7	0.9	24.3	1.3	20.2	1.2	5.8	1.0	4.6	16.2	1.0	3.1	7.6	3.3	6.7	0.3	42.5
2.1% Ga/ZSM-5-R	0.8	1.0	1.1	23.3	1.4	19.9	1.5	5.8	1.4	4.5	16.6	1.1	3.2	8.0	3.4	6.9	0.4	43.7
2.1% Mo/ZSM-5-R	0.6	1.1	1.0	24.0	1.3	18.2	0.9	5.1	1.2	4.9	17.5	1.2	3.6	8.2	3.6	7.3	0.3	46.2
(b)																		
0.8% Zn/ZSM-5	0.9	0.5	1.7	10.0	2.1	15.6	1.7	9.4	2.0	4.5	22.9	1.5	3.9	10.0	4.2	7.2	1.9	54.2
5.1% Zn/ZSM-5	1.4	0.3	2.7	4.3	3.8	10.0	2.8	7.3	2.7	4.1	25.9	2.5	5.3	12.1	4.6	7.0	3.3	61.4
9.0% Zn/ZSM-5	1.3	0.3	2.7	4.6	4.0	10.9	2.9	8.4	3.2	3.7	24.6	2.5	5.1	11.8	4.3	6.7	3.1	58.7

[a]Reaction condition: 0.1 MPa, 450 °C, WHSV 3.88 h^{-1}, time-on-stream =3 h. [b]C_{6-9} alkenes. [c]Benzene. [d]Toluene. [e]Ethylbenzene. [f]*para*-Xylene. [g]*meta*-Xylene. [h]*ortho*-Xylene. [i]C_9 and C_9^+ aromatics. [j]Total yield of aromatics.

$$X_{\text{isobutene}} = \frac{m_{\text{inj isobutyl alcohol}} \times \left(\frac{M_{\text{isobutene}}}{M_{\text{isobutyl alcohol}}}\right) - m_{\text{det isobutene}}}{m_{\text{inj isobutyl alcohol}} \times \left(\frac{M_{\text{isobutene}}}{M_{\text{isobutyl alcohol}}}\right)} \times 100\% \quad (2)$$

$$\text{Sel}_i(\text{wt}) = \frac{m_i}{\sum m_{\text{det } C_xH_y} - m_{\text{det isobutene}}} \times 100\% \quad (3)$$

$$Y_i(\text{wt}) = X_{\text{isobutene}} \times \text{Sel}_i \quad (4)$$

in which M and m represent the molecular weight and weight, respectively.

The water product is not included in the calculations. The detected products refer to hydrocarbons and hydrogen (C_xH_y). Typically, carbon balances are 85−91% over the *x*Zn/ZSM-5 catalysts and 90−95% over the other catalysts, respectively. In the experiments, the conversions of isobutyl alcohol are always close to 100% (>99.99%), and the concentration of isobutene is less than 2 wt % in the detected products for ZSM-5 zeolites, *x*M/ZSM-5, and *x*M/ZSM-5-R (i.e., $X_{\text{isobutene}}$ > 98 wt %, and $X_{\text{isobutene}}$ is not provided in the following Table 1 and 2). Considering these conditions, the yield is approximately equivalent to the selectivity on these catalysts.

3. RESULTS AND DISCUSSION

3.1. Transformation of Isobutyl Alcohol over Purely Acidic Zeolites. Several typical zeolites, including USY, ß, ZSM-11, and ZSM-5, were studied in the transformation of isobutyl alcohol at 450 °C. All these zeolites show high isobutyl alcohol conversions (>99.9 wt %); however, the product spectra are quite different (Table 1). The large pore zeolite of USY[4.3] provides isobutene (52.9 wt %) and butene isomers (27.2 wt %) as the major products, whereas gives very low yield to aromatics (2.5 wt %). Such a product spectrum indicates the dominance of dehydration and sequential isomerizations over the USY zeolite.

dx.doi.org/10.1021/cs300048u | ACS Catal. 2012, 2, 1203−1210

Another large-pore zeolite of ß[31.6] gives a more average product distribution, which consists of propene (19.4 wt %), butane isomers (11.4 wt %), butene isomers (18.1 wt %), C_5 fragments (16.3 wt %), and aromatics (15.0 wt %). As a sharp comparison, ZSM-5[13.3] shows superior performance in the aromatization of isobutyl alcohol, whose aromatics yield achieves 41.6 wt % (BTX 32.9 wt %). The major gas phase products are not isobutene and butene isomers, but saturated propane (22.1 wt %) and butane isomers (21.3 wt %). Similarly, ZSM-11[26.6], another type of pentasil zeolite, also gives aromatics (BTX 31.3 wt %), propane (20.7 wt %) and butane isomers (21.4 wt %), as the main products. Considering the superior catalytic performance, ZSM-5 zeolite was selected for further study.

ZSM-5 zeolites with different Si/Al ratios were studied in the reaction. As shown in Table 1, yields to aromatics are around 42 wt % on ZSM-5 zeolites whose Si/Al ratios are within 13.3 to 42.7. However, ZSM-5[34.3] exhibits a slightly higher yield of 34.3 wt % to BTX. Although ZSM-5 zeolites show rather high yields to aromatics, a large amount of propane and butane isomers are also generated during the reaction.

3.2. Transformation of Isobutyl Alcohol over *x*M/ZSM-5 and *x*M/ZSM-5-R Catalysts. To improve the yield to aromatics, promoters, which are typically used in short alkanes aromatization, are incorporated into ZSM-5 zeolite. Metal species, including Zn, Ga, Mo, La, Ag, Ni, and Pt, are supported on the ZSM-5[34.3] and screened for the reaction. Dramatic discrepancies are observed in the transformation of isobutyl alcohol (Table 2). Among the incorporated metal components, only zinc species result in the enhanced yield to aromatics. Compared with the purely acidic ZSM-5, 2.3% Zn/ZSM-5 improves the aromatics yield to 59.3 wt % (BTX 49.3 wt %) and gives obviously lower yields for propane (5.5 wt %) and butane isomers (12.0 wt %).

In addition to the variations of aromatics and alkanes, a large amount of hydrogen (3.0 wt %) is also generated over 2.3% Zn/ZSM-5. This is indicative of the promoted desorption of H_2 during the aromatization reactions. However, such promotional effects are not observed on the other supported *x*M/ZSM-5. As shown in Table 2a, 2.1% Ga/ZSM-5, 2.4% La/ZSM-5, and 2.1% Mo/ZSM-5 show 42.9, 43.6, and 42.0 wt % aromatics yields, respectively, which are close to the 42.3 wt % aromatics yield on the purely acidic ZSM-5[34.3]. It is also worth noting that the reduced *x*M/ZSM-5-R catalysts do not exhibit remarkably improved catalytic performances. Their yields to aromatics are close to the values of the unreduced counterparts, except for the slight enhancement to 46.2 wt % on 2.1% Mo/ZSM-5-R. In particular, Ga/ZSM-5-R, which is a superior catalyst in the aromatization of short alkanes,[2,15,20] barely promotes the overall aromatization of isobutyl alcohol. Analogously, the yields to aromatics of 2.3% Ag/ZSM-5 and 0.4% Pt/ZSM-5-R are similar to that of ZSM-5[34.3]. Much worse reaction results are observed on 2.2% Ni/ZSM-5-R, which achieves an only 20−50% carbon balance during the initial reaction period due to the severe coking (Supporting Information Table S2). The inferior catalytic performances of *x*M/ZSM-5 and *x*M/ZSM-5-R are still characterized by the high yields to short alkanes and small portion of hydrogen (0.2−0.4 wt %).

The catalytic performances of Zn/ZSM-5 catalysts with different Zn loadings were also studied. As shown in Table 2b and Figure 1a, the yield to aromatics is obviously enhanced with the increase in Zn loading in the low loading range (<2.3 wt %). After that, only a slight enhancement is observed with higher Zn loading; and the highest aromatic yield of 61.4 wt % is obtained on 5.1% Zn/ZSM-5. However, a further increase in Zn loading leads to a descending trend in aromatization, as shown by the 58.7 wt % aromatic yield over 9.0% Zn/ZSM-5. For Zn/ZSM-5 catalysts, the enhancement in aromatics yield is mainly due to the improved formation of toluene and xylene (Figure 1a). In contrast, the yield to benzene is barely improved on these Zn/ZSM-5 catalysts. Compared with the unpromoted ZSM-5 zeolites, Zn/ZSM-5 catalysts exhibit obviously lower yields to the side products of propane (4−10 wt %) and butane isomers (10−16 wt %). The decrease in propane is more pronounced than that of butane isomers over the Zn/ZSM-5 catalysts (Figure 1b). All the catalysts show yields similar to the cracked product of C_1−C_2 (3−4 wt %).

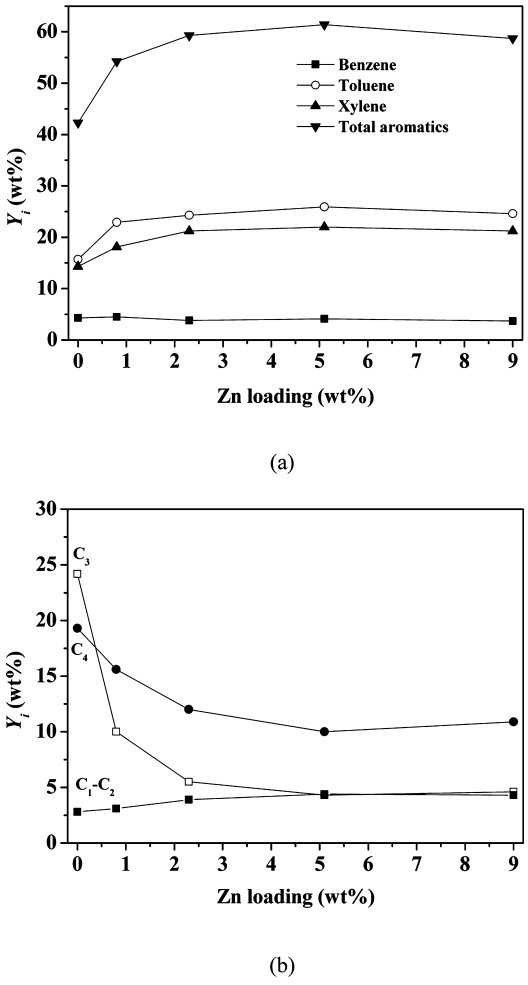

Figure 1. Product distributions as a function of Zn loading. Reaction conditions: 0.1 MPa, 450 °C, WHSV 3.88 h^{-1}, time on stream = 3 h.

Figure 2a illustrates the variation of aromatics yield at the initial stage of isobutyl alcohol transformation. Neither induction period nor dramatic deactivation is observed on ZSM-5 and Zn/ZSM-5 catalysts during the evaluated 5 h. The stable aromatic yields indicate the achievement of steady state of the reaction on these catalysts. A long-term stability test is further studied on 2.3% Zn/ZSM-5. As shown in Figure 2b, the product distributions are relatively stable with the extending time on stream. The yields to aromatics and BTX progressively drop from 59.6 to 56.8 wt % and from 49.7 to 46.3 wt %, respectively. The relatively constant yields to various products

dx.doi.org/10.1021/cs300048u | *ACS Catal.* 2012, 2, 1203−1210

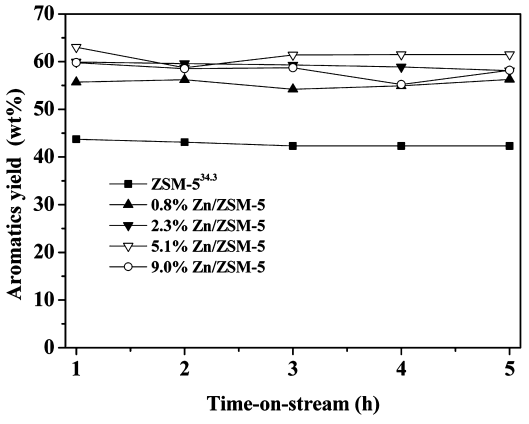

(a)

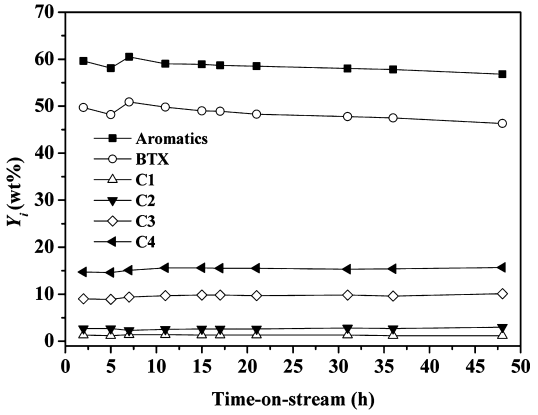

(b)

Figure 2. The stability test of various catalysts: (a) Short-term stability test on ZSM-5 and Zn/ZSM-5 catalysts; (b) long-term stability test on 2.3% Zn/ZSM-5. Reaction conditions: 0.1 MPa, 450 °C, WHSV 3.88 h^{-1}.

also prove the smooth running of the reaction network during the evaluated 48 h.

3.3. Characterization of ZSM-5 and *x*Zn/ZSM-5 Catalysts. In DRIFT IR spectra (Figure 3), the intensity of the band at 3610 cm^{-1}, associated with bridging OH groups,[21−23] is reduced on the Zn/ZSM-5 catalysts. This

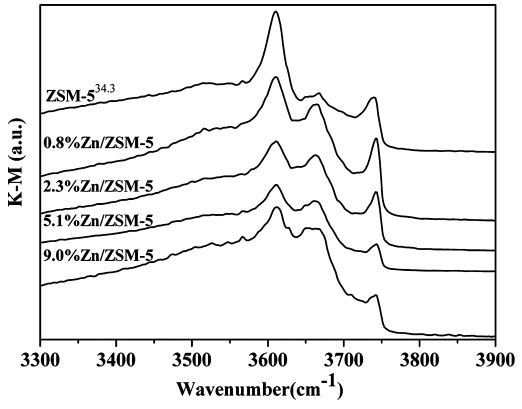

Figure 3. DRIFT spectra of ZSM-5 and Zn/ZSM-5. The samples were pretreated in N_2 at 300 °C for 1 h and cooled to 30 °C.

evidences the decrease in the Brønsted acidity due to the exchange of protons by Zn cations.[16,23] Nevertheless, the 3610 cm^{-1} band still remains on 5.1% Zn/ZSM-5 and 9.0% Zn/ZSM-5, although their Zn loadings are distinctly higher than the theoretical exchange capacity of 1.5 wt % for ZSM-$5^{34.3}$ (page S8 in the Supporting Information). This indicates that only part of the bridging OH can be exchanged by Zn cations.[23,24] The exchange level of Zn/ZSM-5 is estimated by comparing the intensities of 3610 cm^{-1} band (page S9 in Supporting Information). The exchange level increases from 33% for 0.8% Zn/ZSM-5 to 61% for 2.3% Zn/ZSM-5, and maintains this level (61%) for 5.1% Zn/ZSM-5. However, a decreased exchange level of 47% is obtained for 9.0% Zn/ZSM-5, which may be related to the enhanced aggregation of Zn species (vide infra). As shown in Py-IR spectra (Figure 4b), the

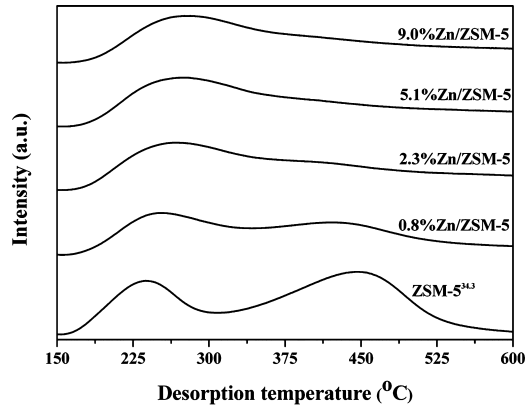

(a)

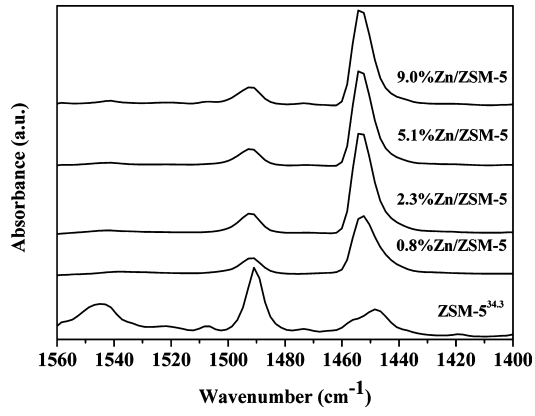

(b)

Figure 4. NH_3-TPD curves (a) and Py-IR spectra (b) of parent ZSM-5 and Zn/ZSM-5 catalysts.

band at ~1550 cm^{-1} on ZSM-$5^{34.3}$ evolves into the negligible ones on Zn/ZSM-5 catalysts. Combined with the diminished desorption peak centered at 450 °C in NH_3-TPD curves, it can be deduced that Zn cations preferentially replace the strong-strength Brønsted acid sites of ZSM-5. Therefore, the remaining bridging OH groups on Zn/ZSM-5 are mainly attributed to the weak-strength Brønsted acid sites. A portion of the incorporated Zn cations also acts as the Lewis acid sites[21,22,25] and gives rise to the widened desorption peak at 230

dx.doi.org/10.1021/cs300048u | *ACS Catal.* 2012, 2, 1203−1210

°C in NH_3-TPD and simultaneously enhanced 1450 cm^{-1} band in Py-IR spectra.

The consumption of bridging OH groups (DRIFT IR and Py-IR) suggests the presence of Zn species at the exchange sites on all Zn/ZSM-5 catalysts. However, it has been reported that Zn/ZSM-5 catalysts prepared by the impregnation method contain exchanged Zn cations, highly dispersed Zn clusters, and ZnO crystallites.[16,23] As shown in UV−vis spectra (Figure 5), a

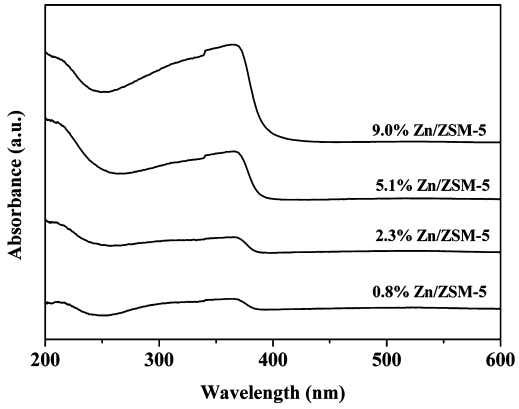

Figure 5. UV−vis absorption spectra of Zn/ZSM-5 catalysts.

weak band appears at ~370 nm on 0.8% Zn/ZSM-5, corresponding to the ZnO crystal on the external surface of ZSM-5.[24,26] This band obviously develops with the increase in the Zn loading. The intensive band on 5.1% Zn/ZSM-5 and 9.0% Zn/ZSM-5 is indicative of the formation of large ZnO particles, which are also clearly observed in the TEM images (Supporting Information Figure S7). For 9.0% Zn/ZSM-5, the characteristic peaks of ZnO crystallites (2θ = 31.7, 34.4, 36.2, and 47.5°) can be observed in the XRD pattern (Supporting Information Figure S3).

3.4. Discussion. The transformation of isobutyl alcohol to aromatics proceeds through the consecutive reactions of dehydration and aromatization. Dehydration of isobutyl alcohol is catalyzed by mildly acidic alumina, metal oxides, and zeolites, which has been studied for decades.[11] Isobutyl alcohol readily undergoes dehydration over the acidic zeolite catalysts (almost 100%) at 450 °C in this work; however, only zeolites with MFI and MEL topologies show high yields to aromatics (Table 1). The aromatization of isobutene and butene isomers (i.e., the products after dehydration of isobutyl alcohol) has been the subject of several studies.[27−29] It has been widely proved that the pore structures of MFI and MEL are in favor of the formation of aromatics and constrain the formation of carbonaceous deposits.[2,3] This is applicable to explain the superior aromatization activities of ZSM-11 and ZSM-5 zeolites in the transformation of isobutyl alcohol.

The conversion of hydrocarbons to aromatics is complicated and involves a complex reaction network and dozens of intermediates. As a simplified model for alkenes, the aromatization primarily consists of oligomerization, cyclization, and the essential dehydrogenation steps paralleled with a sequence of hydrogen transfer reactions.[2−4,30] Accordingly, Scheme 1a describes the major reaction pathways for the conversion of isobutyl alcohol to aromatics over the ZSM-5 zeolites. Starting from isobutyl alcohol, aromatics are formed through the steps of dehydration, oligomerization, cyclization, and the parallel hydrogen transfer reactions. Butane isomers (19−21 wt %) are generated at the expense of isobutene and butene isomers as the balanced products of aromatics due to the hydrogen transfer reactions. Another major balanced product of propane is generated through the combined oligomerization−cracking and hydrogen transfer of C_6−C_9 oligomers. As listed in Table 1, the yield of propane is

Scheme 1. Transformation Pathways of Isobutyl Alcohol over ZSM-5 and Zn/ZSM-5 Catalysts

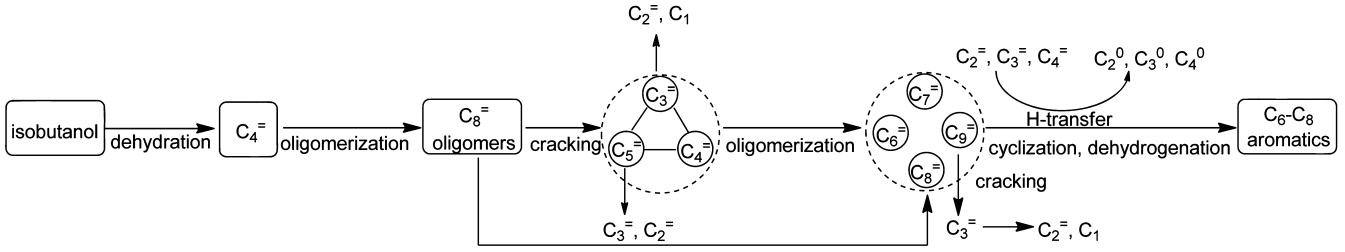

(a) Transformation of isobutanol over purely acidic ZSM-5 zeolites

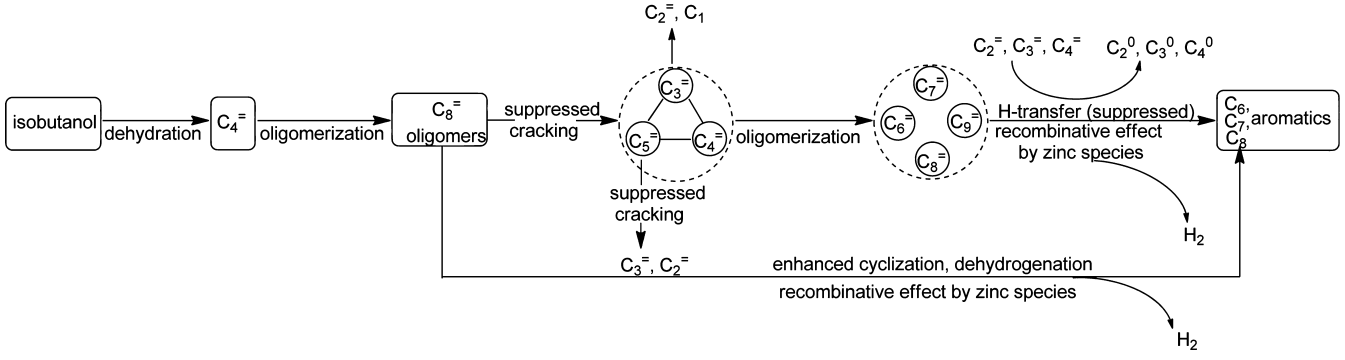

(b) Transformation of isobutanol over Zn/ZSM-5 catalysts

dx.doi.org/10.1021/cs300048u | ACS Catal. 2012, 2, 1203−1210

disproportionally higher than that of methane, indicating that propane does not originate from the protolytic cracking of isobutene or butene isomers. Moreover, the obviously high portion of propane (22−25 wt %) is supportive for the occurrence of multiple oligomerization−cracking ($C_4 + C_4 \rightarrow C_8 \rightarrow C_5 + C_3$; $C_5 + C_4 \rightarrow C_9 \rightarrow C_3 + C_6 \rightarrow 3C_3$). Nearly equimolar ratios are obtained for CH_4/C_2H_4 (Supporting Information Figure S2) over the ZSM-5 and *x*Zn/ZSM-5 catalysts. This suggests that mainly the secondary cracking reactions contribute to the formation of methane and ethene ($C_3 \rightarrow$ H−transfer, cracking $CH_4 + C_2H_4$). Among the above reaction pathways, the intensive multiple oligermization−cracking and hydrogen transfer reactions lead to the formation of undesired saturated C_3^0 and C_4^0 fragments and, thus, limit the aromatization of isobutyl alcohol over the purely acidic ZSM-5 zeolites.

Zn/ZSM-5 catalysts show remarkably improved catalytic performances in these two aspects. As shown in Figure 1, the incorporation of Zn species not only enhances the yield to aromatics but also results in obviously lower yields for propane and butane isomers. The incorporated Zn species may promote the primary aromatization steps (i.e., isobutyl alcohol → aromatics) or give rise to the additional secondary aromatization of the propane and butane isomers (i.e., saturated C_3^0, C_4^0 → aromatics). The analysis of product distribution is informative for such a discussion.

As indicated in Figure 1a, Zn/ZSM-5 catalysts mainly increase the yields of toluene and xylene, which refers to the enhanced formation of C_7 and C_8 oligomeric precursors ($C_4 + C_4 \rightarrow C_8$; $C_8 \rightarrow C_5 + C_3$, $C_3 + C_4 \rightarrow C_7$). This suggests that the multiple oligomerization−cracking of oligomeric intermediates is suppressed, which is due to the decreased strong-strength Brønsted acidity on Zn/ZSM-5, as revealed by DRIFT IR, Py-IR spectra, and NH_3-TPD curves.

In addition to the suppression of multiple oligomerization−cracking, Zn species play a pronounced effect in the essential dehydrogenation reactions of C_7 and C_8 intermediates for the formation of toluene and xylene. Compared with the extremely low portion of H_2 over the ZSM-5, the amounts of generated H_2 are increased by an order of magnitude (19−30) over the Zn/ZSM-5 catalysts (Table 2). The molar ratios of $H_2/(H_2$ + propane + butane isomers) as a function of Zn loading are also calculated (Figure 6). The ratio is remarkably increased from 0.14 for ZSM-5 to 0.66 for 0.8% Zn/ZSM-5 and reaches a plateau around 0.82 after 2.3 wt % Zn loading. This indicates that the dehydrogenation reactions are paralleled with the intensive desorption of H_2 on Zn/ZSM-5 catalysts. Such phenomena have been proposed as the recombinative effect in the aromatization of alkanes, which promotes the dehydrocyclization of alkanes to aromatics on Ga/ZSM-5 and Zn/ZSM-5 catalysts.[2,3,20] As shown in Figure 6, the evolution of $H_2/(H_2$ + propane + butane isomers) ratios follows the variation trend of exchange levels as a function of Zn loading. This correlation suggests that mainly the Zn species residing at exchange sites are responsible for the recombinative effect.

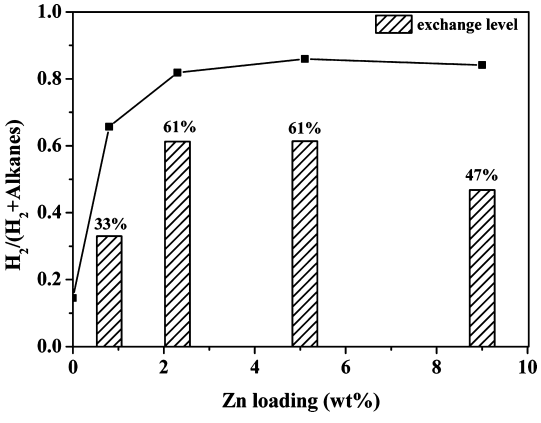

Figure 6. The molar ratios of $H_2/(H_2$ + propane + butane isomers) (recombinative effect/hydrogen transfer) and exchange level as a function of Zn loading.

However, such recombinative effect does not invoke the secondary aromatization of propane and butane isomers (i.e., saturated C_3^0, C_4^0 → aromatics) during the transformation of isobutyl alcohol. As reported, butane is ∼4 times more reactive than propane in the aromatization,[4] which leads to the preferential conversion of butane in the mixed alkanes. However, instead of butane, propane is found to undergo more rapid and substantial reduction in this work (Figure 1b). This disagreement indicates that the improved yields to aromatics are not due to the secondary aromatization over the Zn/ZSM-5.

The promotional effect of Zn/ZSM-5 catalysts on the aromatization of isobutyl alcohol is proposed in Scheme 1b. The incorporation of Zn species preferentially decreases the strong-strength Brønsted acidity of the ZSM-5 zeolites and, thus, suppresses the multiple oligomerization-cracking to the C_3 fragments. Moreover, Zn species residing at exchange sites remarkably enhance the dehydrogenation reactions by the recombinative desorption of H atoms to H_2, which in turn inhibits the hydrogen transfer reactions with C_3^{2-} and C_4^{2-} hydrocarbons.

It is worth noting that the catalytic performances of 2.1% Ga/ZSM-5, 2.1% Mo/ZSM-5, and 2.4% La/ZSM-5 catalyst are very similar to that of purely acidic ZSM-5 (Table 2a). Likewise, the reduced catalysts of 2.1% Ga/ZSM-5-R and 2.1% Mo/ZSM-5-R barely promote the formation of aromatics. The multiple oligomerization−cracking and hydrogen transfer reactions are still intensive on the above-mentioned catalysts, as shown by their product distributions in Table 2. In particular, the reduced Ga/ZSM-5-R does not exhibit the expected promotional effect for the formation of aromatics and H_2 in the transformation of isobutyl alcohol. So far, it is premature to give any confirmative analysis about the inertness of reduced Ga species. We still incline to propose that the presence of a high concentration of water, formed from the dehydration of isobutyl alcohol, is closely related to their inferior catalytic performances. For instance, the oxidation and hydrolysis of reduced Ga species by water vapor with certain partial pressure have been reported on Ga(I)/ZSM-5.[31,32] Further efforts are required to unveil the responsible structure transformation of above-mentioned metal species.

4. CONCLUSIONS

One-step transformation of isobutyl alcohol to aromatics is achieved by ZSM-5 zeolites (Si/Al = 13.4−34.3) at 450 °C under atmospheric pressure. The yields to benzene, toluene, and xylene reach 33−35 wt % over the purely acidic ZSM-5 catalysts; however, large amounts of propane and isobutane are also generated as the balanced byproduct. The aromatization can be enhanced by the incorporation of Zn species. With the suitable Zn loading (2.3−5.1 wt %), the yields to benzene, toluene, and xylene are increased to 49−52 wt %. Mainly the

dx.doi.org/10.1021/cs300048u | *ACS Catal.* 2012, 2, 1203−1210

Zn species residing at exchange sites promote the transformation of isobutyl alcohol in the following two manners: (i) decrease the strong-strength Brønsted acidity of the ZSM-5 zeolites and thus suppress the multiple oligomerization−cracking steps for the formation of C_3 fragments and (ii) facilitate the recombinative desorption of H atoms to H_2 and improve the dehydrogenation reactions for the formation of aromatics. Therefore, the Zn/ZSM-5 catalysts promote the formation of toluene and xylene and inhibit the generation of undesired propane and butane isomers.

■ ASSOCIATED CONTENT

Supporting Information

Solid NMR and TEM characterizations, the schematic diagram of reaction system, the calculated CH_4/C_2H_4 ratios over ZSM-5 and Zn/ZSM-5 catalysts, XRD patterns of Zn/ZSM-5 catalysts, solid NMR spectra of Zn/ZSM-5 catalysts, deconvolution of ^{29}Si spectra, the enlarged region in DRIFT IR for estimation of the exchange level, TEM images of 5.1% Zn/ZSM-5 and 9.0% Zn/ZSM-5, adsorption−desorption isotherms and Horvath−Kawazoe differential pore volume curves of ZSM-5 and Zn/ZSM-5 catalysts, the reported structural variations of reduced Ga species under hydrated conditions, texture properties of various catalysts used in the present study, and the reaction results over 2.2% Ni/ZSM-5-R catalyst. This material is available free of charge via the Internet at http://pubs.acs.org.

■ AUTHOR INFORMATION

Corresponding Author

*E-mail: (S.H.) huangsj@dicp.ac.cn; (L.X.) lyxu@dicp.ac.cn.

Notes

The authors declare no competing financial interest.

■ REFERENCES

(1) Ransley, D. L. In *Kirk−Othrner Encyclopedia of Chemical Technology*, 3rd ed.; Grayson, M., Eckroth, D., Eds.; Wiley-Interscience: New York, 1978; Vol. *4*, p 264.
(2) Bhan, A.; Delgass, W. N. *Catal. Rev.: Sci. Eng.* **2008**, *50*, 19−151.
(3) Caeiro, G.; Carvalho, R. H.; Wang, X.; Lemos, M. A. N. D. A.; Lemos, F.; Guisnet, M.; Ribeiro, F. R. *J. Mol. Catal. A: Chem.* **2006**, *255*, 131−158.
(4) Guisnet, M.; Gnep, N. S.; Aittaleb, D.; Doyemet, Y. J. *Appl. Catal., A* **1992**, *87*, 255−270.
(5) Inui, T.; Makino, Y.; Okazumi, F.; Nagano, S.; Miyamoto, A. *Ind. Eng. Chem. Res.* **1987**, *26*, 647−652.
(6) Huber, G. W.; Corma, A. *Angew. Chem., Int. Ed.* **2007**, *46*, 7184−7201.
(7) Hoang, T. Q.; Zhu, X. L.; Danuthai, T.; Lobban, L. L.; Resasco, D. E.; Mallinson, R. G. *Energy Fuels* **2010**, *24*, 3804−3809.
(8) Szechenyi, A.; Barthos, R.; Solymosi, F. *Catal. Lett.* **2006**, *110*, 85−89.
(9) Anunziata, O. A.; Orio, O. A.; Herrero, E. R.; Lopez, A. F.; Perez, C. F.; Suarez, A. R. *Appl. Catal.* **1985**, *15*, 235−245.
(10) Costa, E.; Aguado, J.; Ovejero, G.; Canizares, P. *Ind. Eng. Chem. Res.* **1992**, *31*, 1021−1025.
(11) Taylor, J. D.; Jenni, M. M.; Peters, M. W. *Top. Catal.* **2010**, *53*, 1224−1230.
(12) Thomas, J. M.; Hernandez-Garrido, J. C.; Bell, R. G. *Top. Catal.* **2009**, *52*, 1630−1639.
(13) Solymosi, F.; Cserenyi, J.; Szoke, A.; Bansagi, T.; Oszko, A. *J. Catal.* **1997**, *165*, 150−161.
(14) Zhang, Y. W.; Zhou, Y. M.; Liu, H.; Wang, Y.; Xu, Y.; Wu, P. C. *Appl. Catal., A* **2007**, *333*, 202−210.
(15) Giannetto, G.; Monque, R.; Galiasso, R. *Catal. Rev.: Sci. Eng.* **1994**, *36*, 271−304.
(16) Biscardi, J. A.; Meitzner, G. D.; Iglesia, E. *J. Catal.* **1998**, *179*, 192−202.
(17) Yin, C. L.; Zhao, R. Y.; Liu, C. G. *Fuel* **2005**, *84*, 701−706.
(18) Chetina, O. V.; Vasina, T. V.; Lunin, V. V. *Appl. Catal., A* **1995**, *131*, 7−14.
(19) Ono, Y. *Catal. Rev.: Sci. Eng.* **1992**, *34*, 179−226.
(20) Biscardi, J. A.; Iglesia, E. *Catal. Today* **1996**, *31*, 207−231.
(21) Kazansky, V. B.; Pidko, E. A. *J. Phys. Chem. B* **2005**, *109*, 2103−2108.
(22) El-Malki, E. M.; van Santen, R. A.; Sachtler, W. M. H. *J. Phys. Chem. B* **1999**, *103*, 4611−4622.
(23) Almutairi, S. M. T.; Mezari, B.; Magusin, P.; Pidko, E. A.; Hensen, E. J. M. *ACS Catal.* **2012**, *2*, 71−83.
(24) Kolyagin, Y. G.; Ordomsky, V. V.; Khimyak, Y. Z.; Rebrov, A. I.; Fajula, F.; Ivanova, I. I. *J. Catal.* **2006**, *238*, 122−133.
(25) Kazansky, V. B.; Subbotina, I. R.; Rane, N.; Van Santen, R. A.; Hensen, E. J. M. *Phys. Chem. Chem. Phys.* **2005**, *7*, 3088−3092.
(26) Chen, J.; Feng, Z. C.; Ying, P. L.; Li, C. *J. Phys. Chem. B* **2004**, *108*, 12669−12676.
(27) Solymosi, F.; Szechenyi, A. *Appl. Catal., A* **2004**, *278*, 111−121.
(28) Choudhary, V. R.; Panjala, D.; Banerjee, S. *Appl. Catal., A* **2002**, *231*, 243−251.
(29) Song, Y. Q.; Zhu, X. X.; Song, Y.; Wang, Q. X.; Xu, L. Y. *Appl. Catal., A* **2006**, *302*, 69−77.
(30) Guisnet, M.; Gnep, N. S. *Appl. Catal., A* **1996**, *146*, 33−64.
(31) Kazansky, V. B.; Subbotina, I. R.; van Santen, R. A.; Hensen, E. J. M. *J. Catal.* **2005**, *233*, 351−358.
(32) Hensen, E. J. M.; Pidko, E. A.; Rane, N.; van Santen, R. A. *Angew. Chem., Int. Ed.* **2007**, *46*, 7273−7276.